IS POLYVINYLIDENE DIFLOURIDE (PVDF) FILM BIOCOMPATIBLE IN THE MURINE COCHLEA?

A thesis submitted in partial fulfillment of the
Requirements for the degree of
Master of Science

By

ROBERT MAXWELL JAGGERS
B.S., University of Tulsa, 2012

2015
Wright State University

WRIGHT STATE UNIVERSITY

GRADUATE SCHOOL

AUGUST 12, 2015

I HEREBY RECOMMEND THAT THE THESIS PREPARED UNDER MY SUPERVISION BY Robert Maxwell Jaggers ENTITLED Is Polyvinylidene diflouride (PVDF) film biocompatible in the Murine Cochlea BE ACCEPTED IN PARTIAL FULFILLMENT OF THE REQUIREMENTS FOR THE DEGREE OF Master of Science.

Robert Goldenberg, MD
Thesis Director

Christopher Wyatt, Ph.D.
Interim Department Chair
Department of Neuroscience, Cell Biology and Physiology

Committee on
Final Examination

Greg Boivin, DVM

Larry Ream, Ph.D.

Robert E. W. Fyffe, Ph.D.
Vice President for Research and
Dean of the Graduate School

ABSTRACT

Jaggers, Robert Maxwell. M.S. Department of Neuroscience, Cell Biology and Physiology, Wright State University, 2015. Is Polyvinylidene diflouride (PVDF) film biocompatible in the Murine Cochlea?

Polyvinylidene fluoride (PVDF) film, a biomaterial that is an integral part of a Totally Implantable Sustainable Hearing Aide (TISHA) device, was examined to determine its biocompatibility within the murine cochlea. The biofilm was implanted in the ear using a round window cochleostomy in 7-9 week old male C57BL/6 mice. Three test groups containing seven mice each were implanted with PVDF film. Each mouse received a sham surgery on the non-implanted cochlea. Three test groups were examined at 48 hours, 3 weeks, and 3 months. At the end of this time the mouse was euthanized, the tissue containing the cochlea was extracted, decalcified in cal-rite solution, processed through a gradient of alcohols and xylene and embedded in paraffin. Slides were made and stained with Hemotoxylin and Eosin. The degree of the Foreign Body Reaction (FBR) in the cochlea with the implanted biofilm was determined quantitatively and qualitatively using nonparametric and parametric tests.

We found that quantitatively the amount of erythrocytes significantly decreased between the 48 hour and 3 week survival length groups (1-way ANOVA, P-value=.020). The amount of neutrophils significantly decreased between the 48 hour and 3 week (1-way ANOVA, P-value=0.22) and 48 hour and 3 month survival length

groups (1-way ANOVA, P-value=0.28). Membrane formation around the implant and presence of foreign body giant cells (FGBCs) and fibrocytes were evident in the chronically implanted animals (≥ 3 weeks). Damage to inner and outer hair cells of the Organ of Corti was observed in both implanted and control cochlea. Angiogenesis, a normal phase of the healing process, was significant only in the 3 week survival group (Fisher's exact test, P-value=.0002).

Animals were assigned individual scores that were related to a certain intensity level of the FBR. There was a significant increase in the average score of the FBR between the 48 hour and 3 week survival length group (Kruskal-Wallis test, P-value=.030). The majority of animals were assigned the lowest intensity level, very mild, while 3 animals received a mild intensity rating.

We determined that PVDF film was biocompatible based on the observation that acute responses of the FBR decreased after the initial time of implantation, chronic response of the FBR did not progress in intensity after the 3 week time point, the average rank of the FBR was the lowest score on our intensity scale, and the components of the FBR did not spread from the site of implantation into surrounding areas of the cochlea. PVDF film did not interrupt the healing process of the host such as the clotting mechanism or become extruded from the cochlea.

This work appeared in abstract form at the Celebration of Research, Scholarship, and Creative Activities 2015 and Ohio Miami Valley Chapter of the Society for Neuroscience, Neuroscience day 2015.

TABLE OF CONTENTS

LIST OF FIGURES

Figure Page

LIST OF TABLES

Table Page

ACKNOWLEDGEMENTS

This research would not be possible without the involvement of several individuals. Firstly, I would like to thank my thesis advisor, Dr. Goldenberg, for giving me this incredible opportunity that has definitely been a major highlight of my academic career. Secondly, I want to extend a thank you to my thesis committee members. Dr. Ream for his guidance and support throughout my tenure in the Anatomy Master's program and Dr. Boivin for his input and guidance in interpreting histological sections, troubleshooting animal surgeries setbacks, and teaching me the valuable lesson that if you focus too much on the little details and don't think about the overall goal you'll "miss the forest for the trees."

I would like to thank Dr. Dudley for her assistance and guidance with the administration of rodent anesthesia, and all of the staff of LAR for never getting tired of the endless amount of questions I asked no matter if it was on a Wednesday afternoon or Sunday morning. I want to extend thanks to Dr. Hansen, Barbara Robinson, and Murat Salihoglu for first showing me the intricacies of the round window cochleostomy surgical procedure. This project would not be possible without funding provided by the Wright State Foundation and the Department of Neuroscience, Cell Biology, and Physiology. Last but not least, I would like to thank my parents, siblings, and grandparents. Whether I live 1.5 hours or 11.5 hours away, I will always appreciate the amount of support and encouragement you give me in whatever I do and wherever I go.

For my parents.

I. INTRODUCTION

A medical material, prosthesis, or device is defined as biocompatible if it resides in an organism with the absence of prolonged damage to host tissue or interruption of normal physiological mechanisms. Biocompatible materials and devices are used extensively in several disciplines; electrode arrays designed to record neural signals from the brain in neuroscience, polymer capsules that deliver a drug to a specific area of the body in medicine, or even gold alloys and porcelain polymers used for dental reconstruction (Davis, 2003). Cell lineages have also been combined with collagen to be used as grafts for integument and bone repair or replacement (Hollinger, 2012). Dermagraft (Organogensis, MA), a mesh-like material that mimics the extracellular matrix of the cellular ultrastructure, was designed to assist the body during skin regeneration after injury (Hollinger, 2012). In addition to the aforementioned definition, a biomaterials main functional role is to replace, monitor, enhance, or diminish a certain tissue, organ or physiological mechanism (Black, 1999).

One area of biomedical research has focused on constructing devices designed to ameliorate deficits in the auditory system. These biomaterials are used as replacements for anatomical structures of the ear, initiators of drug delivery systems used to treat hearing loss, and implanted devices that replicate the physiological mechanism of the auditory pathway.

Damage to the auditory ossicles of the middle ear following chronic disease states can impair or negate vital steps in the auditory pathway. Chronic suppurative

otitis media (CSOM), a chronic infectious disease that is a cause of hearing impairment, can be corrected by auditory ossicle replacement. The Goldenberg hydroxyapatite implant system can be used as a total or partial ossicular bone prosthesis. (Goldenberg and Driver, 2000). Hydroxyapatite, an established biomaterial, is a porous, ceramic compound that resembles human bone (Goldenberg and Driver, 2000). In recent years, cortical bone has also been shown to be a possible biomaterial that can be used for auditory ossicle replacement (Malhotra et al., 2014). Platinum, a known biomaterial that has been incorporated into several prosthesis designs, is also a common material used to replace auditory ossicles (Shah et al., 2013). These approaches are designed to treat deficits attributed to conductive hearing loss.

A relatively new approach at treating sensorineural hearing loss is through the use of a drug delivery system that targets the source of the malady in the cochlea (Nakagawa, 2007). Sensorineural hearing loss can arise from damage to the Organ of Corti, the area of the cochlea that contains the main cellular receptors for hearing, or the neuronal connections between the cochlea and the auditory cortex located in the cerebrum (Inaoka et al., 2011) (Isaacson et al.,2003). Micro-implants made of silicone have been shown to deliver steroids, such as beclamethasone, to cochlear fluids without causing damage to histological or functional aspects of the cochlea (Nakagawa, 2007). The intended result of steroid therapy in the cochlea is to decrease inflammation that is a result of damage to cochlear structures.

Another current method for treating severe to profound hearing loss arising from nerve deafness is through cochlear implant devices. These devices replace a

specific step in the auditory pathway by converting auditory stimuli into electrical impulses. The electrical impulse transfers sensory information to the vestibulocochlear nerve, cranial nerve VIII (Wilson and Dorman, 2008). Damage can arise from many different sources including bacterial infections, pharmaceutical agents, geriatric deficiencies, and exposure to loud noises (Wilson and Dorman, 2008). The cochlear implant (CI) is an example of a current implantable device used to treat auditory deficiencies. CIs replace the function of the sensory epithelium, known as hair cells, located in the cochlea (Wilson and Dorman, 2008). A CI has both external and internal components; a power source, microphone, and speech processor are located externally and involved in the conversion of sound waves into electrical energy that is then transferred to an electrical array located internally within the cochlea (Wilson and Dorman, 2008). The electrode array circumvents the damaged sensory hair cells of the cochlea and stimulates the auditory nerve. The study discussed in this paper examines a material that performs this function and is an integral part of a newly designed cochlear implant device.

Our study analyzed the biocompatibility of polyvinylidene difluoride (PVDF) film when implanted in the mouse cochlea. PVDF film is an integral part of a Totally Implantable and Sustainable Hearing Aid (TISHA) device. The foundation of the TISHA device is built upon principles used in the CI. The device, currently in the experimental stage, is composed of a completely internal structure that is implanted in the cochlea. Biocompatibility will be assessed through the analysis of cochlear histological reactions to the implanted film which will determine the intensity level of the Foreign Body Reaction (FBR).

Biocompatibility Testing

Before a device can be deemed suitable for human use, the reaction of viable tissue to the materials that are used in the device must be established using biocompatibility studies. Biocompatibility testing incorporates *in vitro* and *in vivo* examinations to determine the degree of cytotoxicity, infection, immunogenicity, hemocompatibility, and inflammation to verify one basic principle of the test material: Is the material compatible with different cell lineages and tissues.

One of the initial objectives of material biocompatibility examinations involves *in vitro* cellular trials to evaluate the degree of cytotoxicity. Cytotoxicity evaluation is performed to establish if leachable particulates that accumulate over the life span of the implant are harmful to viable tissue (Silver and Doilon, 1989). Time constrained assays combine a biomaterial with different cell lineages to analyze levels of necrosis and overall viability of the cells with the use of vital stains (Silver and Doilon, 1989). A 2010 study conducted by Shintaku and colleagues examined the *in vitro* compatibility of the components of an implantable artificial cochlea. The implantable artificial cochlea is chiefly composed of PVDF, trifloroethylene (TrFe), silicon, and platinum (Shintaku et al., 2010). Cell cultures combining *Rattus rattus* cerebral cortex neurons with the artificial cochlea materials were created with cell adhesion factors made from human fibronectin. Bovine collagen was used to adhere the neurons to the implant surface (Shintaku et al., 2010). After applying fluorescent Nissl stains to neuronal sections, fluorescent microscopy confirmed that the cultured neurons were viable and showed axonal and dendritic outgrowths. This led them to conclude that PVDF film combined with the three artificial cochlea materials, were non-cytotoxic

(Shintaku et al., 2010). A previous study analyzed the cytotoxicity and hemocompatibility *in vitro* of polyethylene terephthalate (PET) fabric coated in PVDF (Joseph et al., 2008). Sections of PET coated in PVDF were placed in direct contact with L-929 fibroblast cells, whole blood mounts, and human endothelial cells. Observations showed that the PVDF material did not adversely affect viability of the cell linages.

Once a material has been shown to be non-cytotoxic it is incorporated into *in vivo* studies. *In vivo* animal studies can measure the compatibility of a material to different tissue types, such as blood or bone, in a viable organism. Acute and chronic treatments are utilized to measure the amount of irritation, inflammation, and if infectious agents are present. Unresolved chronic inflammation can not only be detrimental to the host, but also compromise the function of the biomaterial (Silver and Doilon, 1989). Histological analysis utilizing light or electron microscopy is an effective technique to quantify the degree of inflammation, both acutely and chronically, along with fibrotic capsule formation in harvested tissue containing the implanted material (Anderson, 2001). A previous study conducted by Gerullis and colleagues compared the *in vivo* host reaction to PVDF film mesh and two other polymer meshes. When harvested at different time points, the short term implanted PVDF film showed signs of macrophage infiltration and exudate associated with the acute inflammatory response (Gerullis et al., 2014). When compared to the two remaining polymer meshes, PVDF film had the lowest long term levels of measured components of chronic inflammation such as connective tissue and angiogenesis formation at the site of implantation (Gerullis et al., 2014). The study noted that even

though PVDF mesh showed the lowest levels of inflammation in the chronic implant group, PVDF film had the highest level of macrophage infiltration acutely among the three mesh implants.

After the biocompatibility of a material has been established in the presence of different cell lineages and within an animal model the next step is clinical trials involving human participants. Clinical trials incorporate several steps known as phases and involve a completely designed material or device that is implanted in a human participant under tightly controlled conditions and strict observation. In the case of PVDF film, the clinical trial would be concerned with the performance of the film as a component within the TISHA device. Clinical trials are the final examinations that biomaterials must undergo in order to establish that they can be implanted within the human body (Black, 1999).

Building off past *in vitro* and *in vivo* test results, this study examined the *in vivo*, nonfunctional biocompatibility of PVDF film in the mouse cochlea. Harvested tissue containing the implant material was stained with Hemotoxylin and Eosin and both quantitatively and qualitatively analyzed to measure select parameters of inflammation, such as the amount of inflammatory cells, areas of necrotic tissue, and amount of capsular formation on the surface of the implant (Silver and Doilon, 1989).

Foreign Body Reaction to an Implanted Material

When an external barrier of the body, such as integument or a mucous membrane is subjected to a traumatic event or breached by a foreign object a specific

defense mechanism is elicited by the host. This response to injury, and the overall mechanism of the healing process, is set in motion by an inflammatory response. The inflammatory response is a nonspecific stereotyped reaction by the host to a stimulus that can vary greatly in intensity (Slauson and Cooper, 1982). The inflammatory response can be characterized by four "cardinal signs," calor (heat), rubor (redness), tumor (swelling), and dolor (pain) (Slauson and Cooper, 1982). The mediators of the inflammatory response are blood derived that use vasculature as a conduit to reach the site of injury (Slauson and Cooper, 1982). There are derivations to the inflammatory response that depend on the type and duration of the stimulus. This research is concerned with the type of inflammation that encounters a foreign object implanted in the host.

Infection at the site of implantation can have detrimental effects to the surrounding tissue. Infection can lead to tissue inflammation and changes in cellular structure, most notably hypertrophy and hyperplasia (Silver and Doilon, 1989). Infection can arise from improper sterilization techniques and compounds composed of biomaterials that interrupt the ability of leukocytes to properly function during the inflammatory response (Silver and Doilon, 1989). Infection is the colonization and growth of microorganisms such as bacteria that can be the result of a surgical procedure to implant a biomaterial (Black, 1999). Infection can cause considerable damage to the host and in extreme cases can increase the rate of necrosis, the death of living tissue. Necrotic tissue can be observed in many different states and can result from toxins produced by fungi and bacteria (Cheville, 1988). Peptide

components can be released from necrotic tissue which can instigate inflammation (Cheville, 1988).

The term for the collective processes that are initiated during the implantation of a foreign material in the body is known as the Foreign Body Reaction (FBR). This initial phases of the FBR are set into motion when a foreign material is implanted and establishes an interface with tissue. This is the case even for biocompatible materials that are deemed non-toxic, non-immunogenic, and stable compounds. (Hu et al., 2001) The extent and magnitude of the FBR varies depending on the physical and chemical properties of the material and the overall health, species, and age of the host (Anderson, 2001). These parameters determine the degree of the FBR which can serve as one method to measure the biocompatibility of a material.

The FBR is used to repair and remodel damaged tissue and degenerated cells, recruit specific immune cells to the site of implantation, and seal off and if possible degrade the material that composes the foreign object. The key events of the FBR are illustrated in **Figure 1**. Fibrotic encapsulation resulting from fibrous tissue production will inevitably accompany any foreign object implanted in vascular tissue (Anderson, 2001). Within the first minutes of implantation serum plasma proteins leave the vasculature and are attached and absorbed to the foreign object's surface. The marked increase in permeability in capillary endothelial cells and dilation of capillaries around the site of injury caused by the foreign body can be implemented by vasoactive amines such as histamine and serotonin. Mast cells residing in the tissue are one source of released histamine (Slauson and Cooper, 1982). Erythrocyte accumulation causes edema formation at the site of implantation. Vasodilation and

increased permeability in microvessels provides avenues for the passage of both plasma proteins and circulating leukocytes out of systemic circulation (Slauson and Cooper, 1982). Trauma to vasculature that leads to hemorrhage can also serve as a route for plasma proteins to be exposed to the implant. These plasma proteins create a thin layer around the material. The matrix formed as a result of protein absorption to the material's surface is related to thrombus formation at the site of implantation and is mainly composed of fibrin, endothelial cells, platelets, and inflammatory cells (Anderson, 2001). Fibrinogen is the main plasma protein that contributes to the encapsulation of the foreign object, along with serum albumin and immunoglobins (Hollinger, 2012). The layer created on the material's surface serves as an interface between the object and the body; signaling molecules released from the protein layer recruit inflammatory cells to the site of the foreign object which initiate the preceding steps in the FBR. A previous study has shown that the absorption of the plasma protein fibrinogen to an implant's surface exposes specific protein epitopes that are essential for recruitment of macrophages to the site of implantation (Hu et al., 2001).

Among the attracted inflammatory cells, the two most abundant phagocytic leukocytes are neutrophils and monocytes, the latter giving rise to macrophages. Two main roles of these immune cells are to degrade the foreign material through the production and excretion of enzymes housed in lysosomes and ultimately phagocytize particulates of the degraded foreign body. Enzymes are tailored to specifically degrade certain macromolecules; Cathepsins specifically degrade proteins, Acid Ribonuclease degrades the nucleic acid RNA, Acid Lipase degrades lipids, and Lysozyme degrades carbohydrates (Slauson and Cooper, 1982). The first

inflammatory cells to arrive and degenerate in the shortest amount of time are neutrophils. Neutrophils, along with basophils and eosinophils are classified as a type of leukocyte known as granulocytes. Granulocytes are a distinct class of leukocytes because they contain specific granules. Agranulocytes are the other class of leukocytes that do not contain specific granules. Lymphocytes and monocytes are classified as agranulocytes (Gartner and Hiatt, 2007). Neutrophils are the majority of circulating granulocytes in the blood and during acute inflammation. Neutrophilic enzymes are housed in both specific, azurophilic, and tertiary granules (Gartner and Hiatt, 2007). Within the first few hours of implantation, circulating neutrophils in the blood begin to adhere to luminal side of endothelial cells of vasculature located near the implant. Through a process known as diapedesis, circulating leukocytes exit the blood vessels and pass through gaps created between endothelial cells. Along with signaling factors, changes in the local pH and chemical configuration can chemotactically recruit additional neutrophils to the site of implantation (Black, 1999). Additionally, opsonins, which include antibodies, complement factors, and lysozyme, mark foreign objects and make them more attractive to immune cells through a process known as opsonization (Slauson and Cooper, 1982).

Two mononuclear phagocytes that are recruited to sites of injury are monocytes and macrophages. After exiting the vasculature both cell types migrate to the site of inflammation. Macrophages are attracted to the site of injury by several types of cytokines including macrophage colony stimulating factor (M-CSF) and interferon λ (Black, 1999). Macrophages, found in circulation and also residing in tissue, are the major cell type of chronic inflammation, releasing signaling factors that

dictate many aspects of the healing process such as angiogenesis and recruitment of fibroblasts and additional inflammatory cells to the site of injury (Anderson, 2001).

Fibroblasts, the mitotically active counterpart of fibrocytes, are normally found in wounds and assist in the process of sealing off and separating the foreign material from the rest of the body. Fibroblasts are attracted to the site of implantation through several pathways: platelet-derived growth factor (PDGF) and transforming growth factor β (TGF-β), which are released by platelets, monocytes, and lymphocytes (Anderson, 2001). Matrices of collagen and proteoglycans are formed by fibroblasts around the foreign object (Hollinger, 2012). This avascular tissue, known as granulation tissue, is composed of fibroblasts encased in the secreted extracellular matrix (Silver and Doilon, 1989). The collagen matrix is mainly composed of Type III collagen with Type I being the main component of the matrix as the healing process progresses (Silver and Doilon, 1989). This matrix can also contain vascular growths that give evidence to angiogenesis at the site of implantation (Cheville, 1988). Capillaries are formed as a response to hypoxic conditions, signaling factors from neutrophils, and heparin released from mast cells (Cheville, 1988).

One final cell lineage observed during a FBR is formed from the fusion of monocytes and macrophages. Foreign Body Giant cells (FBGCs) are formed when an encountered foreign object is too large or simply unable to be degraded by a macrophage. One common class of giant cells are Osteoclasts which are found in bone and function in bone resorption (Anderson, 2001). FBGCs are observed in the latter stages of inflammation and are normally found within close proximity to the foreign object. Interleukin 4 (IL-4) is one known activator of FBGs formation released from

macrophages (Anderson, 2001). They have a dual function as immune cells which is to release proteolytic enzymes to degrade the material and signaling factors to recruit inflammatory cells to the site of injury (Hollinger, 2012). Known to be present at the implant surface decades after the initial implantation, FBGCs configuration is dictated by the physical properties of the foreign object. Rough surfaced implants such as Teflon grafts found in vasculature have a greater amount of FBGCs adhering to their surface compared to flat, smooth implants that are normally subjected to only a few layers of FBGCs and accompanying macrophages (Anderson, 2001).

Figure 1.

Illustration of events that comprise the Foreign Body Reaction of the host to an implanted material over time (Grainger 2013).

Figure 1.

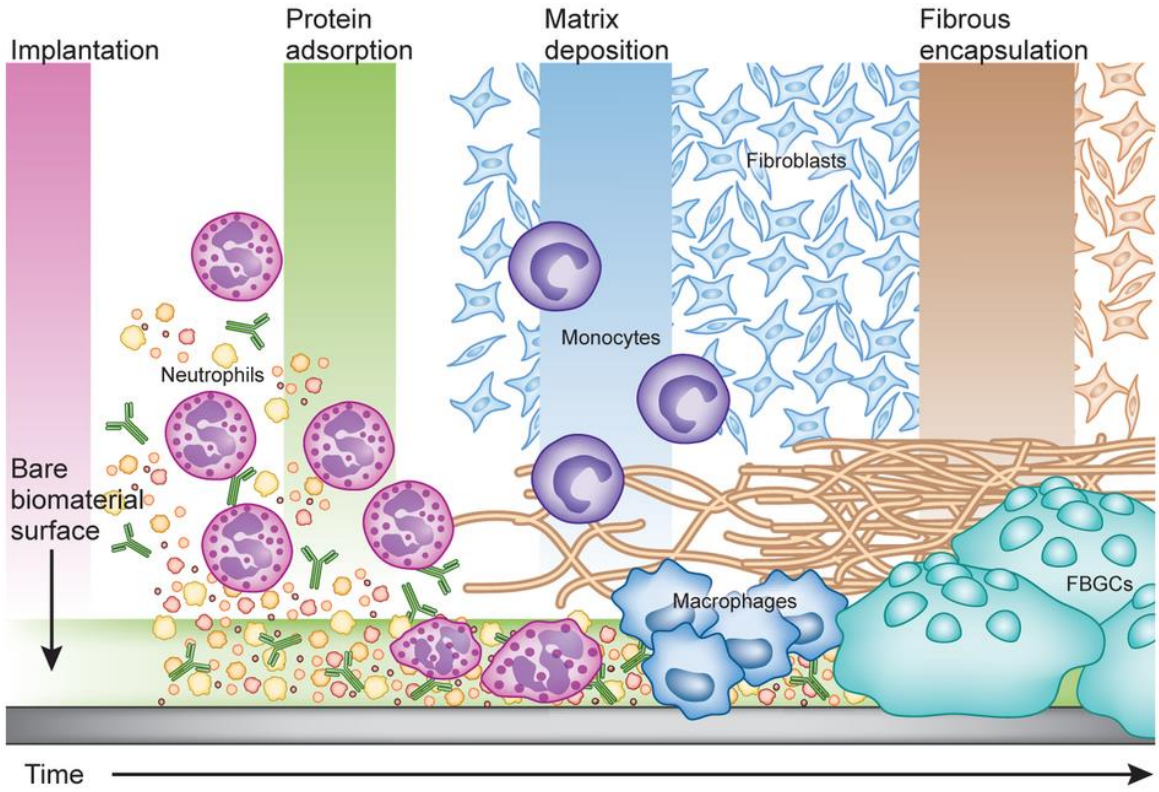
Implantation
Protein adsorption
Matrix deposition
Fibrous encapsulation
Fibroblasts
Monocytes
Neutrophils
Bare biomaterial surface
Macrophages
FBGCs
Time

PVDF film as a component of the TISHA Device

Polyvinylidene difluoride, PVDF, is a translucent, plastic fluoropolymer that has applications across several fields (Piezotech, 2015). PVDF is used in acoustical devices including microphones and sonar equipment. Pertaining to the medical field, PVDF has been used in blood pressure monitors and pressure sensors in artificial skin (Piezotech, 2015). PVDF material is manufactured in a film form because of the materials ability to exist in a solid crystalline phase. One unique property of the PVDF biofilm is its capability to elicit the piezoelectric effect. When combined with a metal polymer, polarized PVDF film will produce an electric charge when subjected to mechanical stress. The addition of a metal polymer allows the static charge produced on the films surface to propagate into an electrical impulse. The piezoelectric effect allows PVDF film to replicate physiological mechanisms that convert mechanical energy into electrical impulses.

The PVDF film is an integral part of a newly designed hearing aid known as the Totally Implantable and Sustainable Hearing Aid (TISHA) device. The concept for the TISHA device came to fruition through a collaboration of researchers from Wright State University (Dayton, OH) and Advratech, LLC (Dayton, OH). The main advantages the TISHA device has over current market hearing aids is its completely internal design with the absence of any external apparatuses (antenna or battery) and the procedure to implant the device into the inner ear will be minimally invasive. **Figure 2** illustrates the structural differences between the cochlear implant and TISHA device. The device will be used to treat hearing loss caused by nerve deafness. The functionality of the device relies on piezoelectric property of the PVDF film. This

characteristic of the film allows the device to replicate the function of the cellular hearing receptors located within the cochlea. A study performed by Inaoka and colleagues concluded that PVDF film is capable of replicating the hearing receptors located specifically in the Organ of Corti of the cochlea in guinea pigs that were subjected to drug-induced deafness.

Figure 2.

Comparison of the physical design and differences of the current CI and TISHA device. Note the absence of external and implanted devices in the TISHA device when compared to the CI (Goldenberg and Zhuang, 2015).

Figure 2.

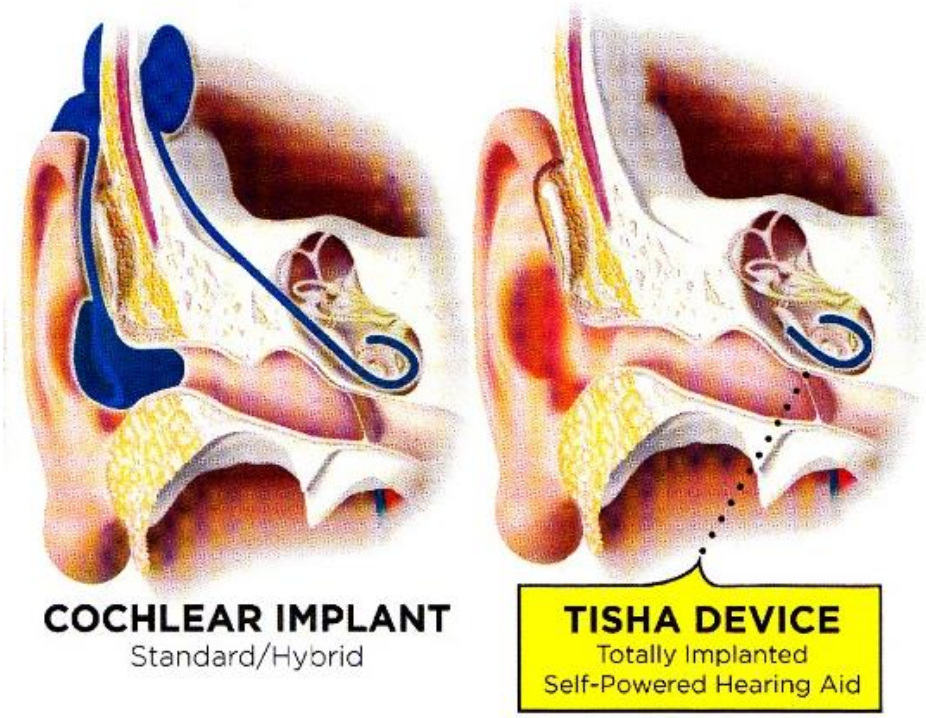
COCHLEAR IMPLANT
Standard/Hybrid
TISHA DEVICE
Totally Implanted
Self-Powered Hearing Aid

Basic Anatomy and Physiology of the Murine Cochlea

Sections of PVDF film were implanted in the mouse cochlea. The cochlea was chosen as the site of implantation because the ultimate use of the biofilm will be as a part of a cochlear implant device. Our animal model was the C57Bl/6 strain of *Mus musculus*. Historically, cat (*Felis catus)* and guinea pig (*Cavia porcellus*) have been the animal model for surgeries involving the auditory system due to the ease of accessing the cochlea surgically (Soken et al., 2013). *M. musculus* has been incorporated into cochlear studies in part due to the accurate modeling of age-related hearing loss as observed in the human population (Soken et al., 2013).

The ear is divided into three regions, the outer, middle, and inner ear. The outer ear is composed of a cartilaginous structure known as the pinna that surrounds the external auditory meatus (Scudamore, 2014). Sebaceous and ceruminous glands are found on both the outer and inner portions of keratinized squamous epithelium of the external auditory meatus (Scudamore, 2014). The external auditory meatus ends at the tympanic membrane, a thin collagenous structure lined with keratinized squamous epithelium located externally and respiratory epithelium internally (Scudamore, 2014).

The middle ear is an air-filled chamber lined with simple squamous epithelium that is located in the petrous portion of the temporal bone (Gartner and Hiatt, 2001). The middle ear houses the three auditory ossicles, the malleus, incus, and stapes. The middle ear is connected to the nasopharynx through the pharyngotympanic tube and the inner ear through the round and oval windows. The footplate of the stapes bone, forms a direct connection with the oval window. The oval window of the cochlea

functions as a conduit for the vibrations produced from sound waves that are transferred from the outer ear to the tympanic membrane and then to the chain of auditory ossicles. The vibrations are transferred from the footplate of the stapes to the oval window of the cochlea which sets in motion the fluid located in the cochlea (Gartner and Hiatt, 2001).

The comparative anatomical features and physiological mechanisms of the cochlea are equivalent among all mammals, including the rodent and human (Forge and Wright, 2002). The internal cochlear structures are illustrated in **Figure 3**. The inner ear can be divided into two labyrinths: a membranous labyrinth that contains a fluid-filled canal that is connected through a series of membranes and an encasing fluid-filled bony labyrinth (Forge and Wright, 2002). The scala media, also known as the cochlear duct is found in the membranous labyrinth and contains an extracellular fluid known as endolymph that is high in potassium ions (K^+) and low in sodium ion (Na^+). The high positive electrical potential of endolymph (+80 mv) is known as the endocochlear potential (EP) (Forge and Wright, 2002). The EP is essential to the transduction of electrical impulses from the Organ of Corti hair cells. The bony labyrinth houses the scala tympani and scala vestibule which both contain perilymph, a fluid that has low K^+ and high Na^+ ionic concentrations that are similar to cerebrospinal fluid (CSF) and extracellular fluid found elsewhere in the body. The difference in ionic composition of the endolymph and perilymph fluids is a critical aspect of physiological mechanism of hearing. The scala tympani and vestibule are joined together at a region near the apex of the cochlea known as the helicotrema (Gartner and Hiatt, 2001). Separating the scala media and scala vestibule is a thin layer

of epithelium known as Reissner's membrane. This membrane functions as a barrier to separate the two distinct ionic concentrations of the fluids in the scala media and scala vestibule. The basilar membrane separates the scala media from the scala tympani (Nolte and Sundsten, 2009). The round and oval windows of the cochlea are separated by the cochlear promontory. The scala tympani ends at the opening of the round window, whereas the scala vestibule ends at the opening of the oval window (Scudamore, 2014).

The scala media houses the Organ of Corti, the area of specialized sensory epithelium in the cochlea. Two groups of cells, known as inner and outer hair cells, are the main receptors for hearing. Spanning the length of the cochlea, the hair cells are organized in rows in the scala media with outer hair cells grouped into 3 rows and inner hair cells grouped into one row (Nolte and Sundsten, 2009). Each type of hair cell has apical membrane projections identified as microvilli, but commonly referred to as stereocilia (Nolte and Sundsten, 2009). The stereocilia are grouped on the apical membrane of the hair cells, arranged in order of increasing height and are connected to each other through intercellular connections at their apexes known as tip links (Nolte and Sundsten, 2009) The outer hair cell stereocilia are embedded in the tectorial membrane located in the scala media while the inner hair cell stereocilia are freely floating in the scala media (Nolte and Sundsten, 2009). Both sets of stereocilia are bathed in the endolymph of the scala media and embedded in the basilar membrane (Forge and Wright, 2002). The rigidity and stiffness of the basilar membrane differ throughout the cochlea. Near the oval widow, at the base of the cochlea, the basilar membrane is less flexible and more rigid compared to the basilar membrane at the

apex of the cochlea, near the helicotrema (Guyton and Hall, 2006). This difference in membrane stiffness accounts for the observation that different portions of the basilar membrane resonate at different sound frequencies (Guyton and Hall, 2006).

The physiological mechanism of hearing is ultimately dependent on the Organ of Corti, specifically inner and outer hair cells, producing an electrical impulse in response to interaction with traveling fluid waves in the cochlea (Forge and Wright, 2002). Once the basilar membrane is set in motion by a traveling wave, the stereocilia, which are coupled to the basilar membrane, change their orientation in the scala media; deflection toward the tallest stereocilia will depolarize the hair cell, while deflection away from the tallest stereocilia will hyperpolarizes the hair cell (Guyton and Hall, 2006). The process of depolarization is initiated by the opening of cationic channels in the stereocilia that allow K^+ ions from the endolymph to enter the hair cell. This sets in motion the process of electrical impulse production which is propagated from the hair cells to cochlear nerves fibers (Forge and Wright, 2002). When the hair cell depolarizes, voltage-gated Ca^{2+} channels open causing an influx of Ca^{2+} into the hair cell and allowing the release of neurotransmitter onto nerve fibers (Forge and Wright, 2002). The neurotransmitter found in vesicles located in the pre-synaptic area of the hair cells has been shown to be glutamate (Nolte and Sundsten, 2009). Outwardly rectifying K^+ channel are found in the hair cell membrane to facilitate the removal of K^+ ions after depolarization. Located alongside the hair cells in the Organ of Corti are several classes of supporting cells, such as Dieter's and Hensen's cells, that provide mechanical support to the hair cells and are also thought to remove excess K^+ ions

found in the intercellular spaces of the sensory epithelium through gap junctions (Forge and Wright, 2002).

An electrical impulse generated by hair cells travels though nerve endings to the cochlear portion of the vestibulocochlear nerve (CN VIII). The spiral ganglion located in the modiolus houses the cell bodies of the cochlear nerve. The spiral ganglion axons travel to two distinct regions found in the medulla, the dorsal and ventral cochlear nuclei (Guyton and Hall, 2006) From the medulla neurons travel contralaterally to synapse on the superior olivary nucleus located in the brainstem (Guyton and Hall, 2006). From the brainstem auditory neurons travel superiorly to the lateral lemniscus of the pons then synapse with the inferior colliculus located in the midbrain until finally terminating in the auditory cortex located in the superior gyrus of the temporal lobe (Guyton and Hall, 2006).

Figure 3.

Cross-sectional view of a 20x objective control animal image. Shown are the 3 fluid filled chambers of the cochlea, scala tympani, scala vestibule, and scala media. Reissner's membrane (RM), the basilar membrane (BM), and tectorial membrane (TB) are identified. Note the position of the stria vascularis (SV) and Organ of Corti (blue box) in in the scala media.

Figure 3.

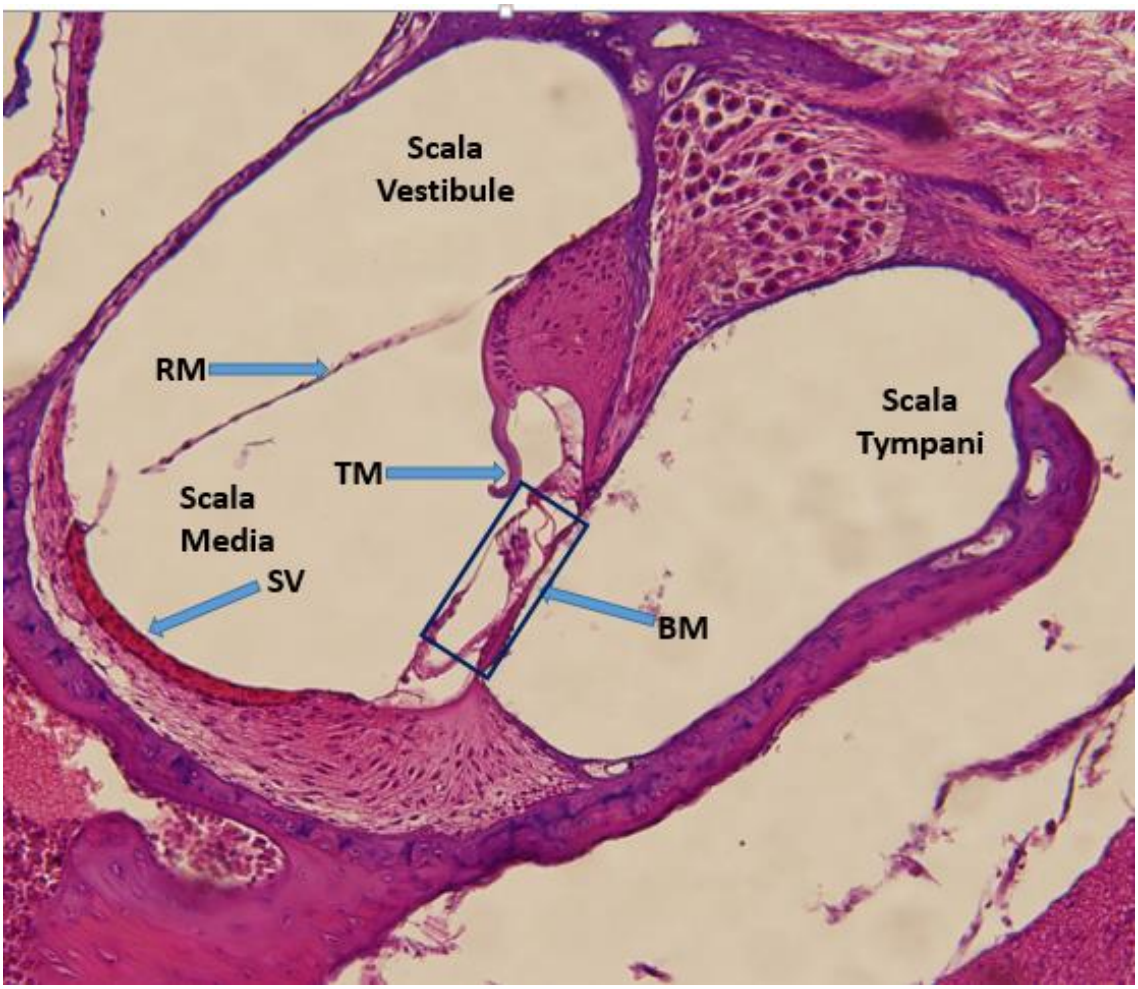

II. MATERIALS AND METHODS

All animal experimental and surgical procedures were conducted in the Laboratory Animal Resource (LAR) facility with approval of the Wright State University Laboratory Animal Care and Use Committee.

Animal Model and Study Design

Adult male C57Bl/6 strains of *M. musculus* (Harlan Laboratories, Indianapolis, IN) ranging between 20-25 grams in weight and 7-9 weeks of age were subjected to a surgical procedure to implant a section of sterile PVDF film within the cochlea. Biocompatibility testing that involves implanted devices implements the use of study groups that differ in the length of contact with viable tissue (Anderson, 2001). There were three groups containing seven mice, all receiving a similar implant and being harvested at either an acute (48 hours), moderate (21 days), or chronic (90 days) time point. The survival length periods were chosen based on Food and Drug Administration (FDA) regulations outlined in the Use of International Standard ISO-10993 for evaluation tests examining the biological effect of implanted devices (www.fda.gov/MedicalDevices). The PVDF film was cut into individual sections under a light microscope using a scalpel blade to the approximate dimensions of 1-2 mm in length and 0.25-0.5 mm in width. Film implants were sterilized pre-operatively in an autoclave. A sham surgery was performed on the contralateral cochlea. Both before and following surgery, animals were housed in individuals cages located in LAR.

Surgical Procedure Overview

The procedure used in the study was adapted from a surgery first performed by Soken et al. (2013). The surgery, known as a round window cochleostomy, accesses the cochlea through one of its two openings, the round window. This innovative procedure accesses the cochlea from a dorsal approach while reducing trauma by sparing surrounding vasculature structures and reducing incision size. A similar surgery uses a larger incision site in the ventral area and cauterizes an artery (stapedial artery) within close proximity of the cochlea.

Each surgery was performed using sterile technique, and instrumentation along with implanted materials which were sterilized in an autoclave before surgery. Prior to surgery, the animal was anesthetized with a Ketamine (100 mg/kg) and Xylazine (10 mg/kg) solution (.1 ml/20 g dosage, intraperitoneal). Artificial tears were applied to both eyes, and the site of incision, caudal to the auricle, was shaved. Three applications of alternating Povidone Iodine scrub and 70% Ethyl Alcohol swabs followed by a single application of Betadine solution were used to aseptically prepare the site of incision. The animal was placed in the prone position in the horizontal plane. A heating pad was used to counteract the excessive decrease in body temperature during the surgery. A surgical microscope (Zeiss, Germany) was used through the extent of the procedure. Anesthesia during the surgery was administered through a nose-cone that delivered a gaseous mixture of isoflurane and oxygen to the animal. With the animal placed in the prone position, a post auricular incision, 1.5-2 cm in length, was made extending through the angle of the mandible (Soken et al. 2013). A retractor was placed in the incision following blunt dissection of the

subcutaneous tissue. The great auricular nerve was located crossing over the surface of the sternocleidomastoid muscle (SCM) and cut. The SCM was cut at its proximal attachment and reflected revealing the tympanic bulla (TB) of the temporal bone with the posterior belly of the digastric muscle (PBD) covering its rostral surface. The TB encloses the bony features of the external acoustic meatus, middle ear, and inner ear (Hajbi-Yonissi et al., 2007). The components of the inner ear enclosed within the rostro-medial portion of the TB are the cochlea, labyrinth and vestibule (Hajbi-Yonissi et al., 2007). The rostral portion of the trapezius muscle was excised to reveal the facial nerve exiting the cranium through the stylomastoid foramen (SF). The superior portion of the PBD covering the TB, located distally to the facial nerve, was removed with a cauterizer (Argent Fine Tip Cautery). Exposure of the RW of the cochlea was achieved through a bullotomy. The burr hole, created using a drill (115 Volt Dremel Drill, Mount Prospect) fitted with a 0.7 mm diamond burr drill bit, was situated in a triangular space illustrated in **Figure 4** and bordered by: 1) the fissure between the mastoid process and tympanic bulla 2) the anterior insertion of the PBD 3) the line joining these two boundaries that crosses the SF (Soken et al., 2013). The drill was operated on a low power setting to insure that the stapedial artery (SA), a branch of the internal carotid artery that travels along the inferior border of the RW before passing through the crura of the stapes in the middle ear, was not ruptured (Mistry et al., 2014). Upon completion of drilling the burr hole, fine tip forceps were used to widen the opening thus allowing easier access to the RW (Mistry et al., 2014). The ventral surface of the animal was rotated forward for a better view of the RW. If still intact, microforceps were used to penetrate and remove the RW membrane.

Evidence of the membrane removal was determined through leakage of perilymph fluid from the cochlea. A sterilized section of PVDF film was inserted into the RW using a pair of micro aural cup forceps. In some instances the width of the film was trimmed in order to fit appropriately. The entire length of the film was inserted into the RW at which point resistance was met due to the decreasing diameter of the cochlea. A section of trapezius fascia was inserted into the RW to secure the biofilm in the cochlea and suppress the flow of perilymph fluid. SCM muscle fibers were then reattached followed by closure of the skin at the site of incision.

Following the procedure, injections of 0.5 ml sterile saline and Buprenorphine (.1 ml/20g dosage) were given to the animal. Three administrations of Carprofen (.1 ml/10 g dosage) were given within the first 72 hours following surgery. The site of incision and overall health of the animal were checked twice daily for the first 48 and once daily for 10 days following the initial 48 hour postoperative period. Any signs of pain encountered post-operatively were relieved with administration of Carprofen. If the animal displayed severe head-tilt, signs of infection around the incision, or weight loss exceeding 20% of pre-operative weight, it was removed from the study. One animal in the 3 month survival length group was removed prematurely from the study due to unresolved tail lesions stemming from dermatitis. Yohimbime (Lloyd Laboratories, Shenandoah, IA) was administered twice postoperatively to aid in recovery from anesthesia.

Figure 4.

Depiction of triangular area where burr hole is placed (Soken et al., 2013). Section of the posterior belly of digastric (PBD) removed that covers lateral portion of tympanic bulla (TB). Superior border of triangle is formed by mastoid process (MP). Facial nerve (CN VII) is shown exiting the temporal bone near proximal portion of triangle.

Figure 4.

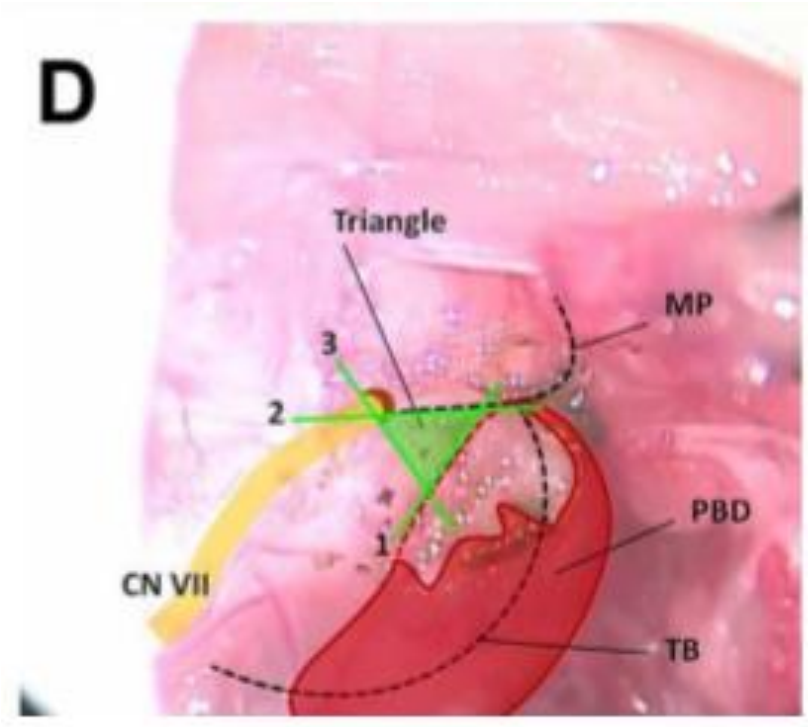

Review of Tissue Extraction, Processing, and Examination

Each animal was euthanized by CO^2 inhalation at a designated time following implantation. The mouse was decapitated and the cranium and surrounding musculature were placed in a solution of Cal-Rite decalcifying solution (Richard-Allen Scientific) for 4-6 days. Once the tissue had been sufficiently decalcified, further dissection was carried out to remove the bones of the cranium and expose only the temporal bone encasing both the right and left cochlea. The tissue was then stored in a solution of 10% neutral buffered formalin until processing through a gradient of ethyl alcohol solutions and xylene. Each sample was embedded in paraffin wax following the processing procedure. The staining and sectioning of each sample was performed by AML laboratories (Baltimore, Maryland). Ten Hemotoxylin and Eosin stained slides were made from each sample. The tissue was cut every 8 microns with an individual section thickness of 5 microns.

Both quantitative and qualitative analyses were used to determine the degree of inflammation in each implanted cochlea. Light microscopy analysis was performed on each slide to determine the degree of inflammation. Each slide was analyzed on objectives ranging from low (2x) to high power (100x). The structural condition of cochlear structures and the composition of cochlear infiltrate was recorded. If inflammation was present histopathological analysis identified certain cell types present which included neutrophils, erythrocytes, FBGCs, and fibrocytes (which included fibroblasts). Individual counts of each cell type in implanted cochlea were performed and compared across treatment groups. The presence of any necrotic tissue and formation of multi-layered membrane was also recorded. If present, the

width of the multi-layered membrane around the biofilm was measured. Qualitatively, the degree of damage to structures within the cochlea was assessed. Damage that existed as an artifact of tissue sectioning was not recorded. The basilar membrane, tectorial membrane, Reissner's membrane, stria vascularis, and the inner and outer hair cells of the Organ of Corti were analyzed to determine if the structure was damaged. The membranes were determined to be damaged if there was a tear or rupture on the apical or basolateral surface. Organ of Corti damage was classified as displacement or degeneration of inner and outer hair cells. Infiltration of erythrocytes into the Organ of Corti was recorded if observed. To determine if the damage to the structures was due to damage from the biofilm or trauma from surgically accessing the cochlea, 3 control cochlea, representing each of the survival length groups, were examined.

The cellular composition of the infiltrate within the cochlea was further analyzed using the image processing program, Image J (NIH, Bethesda, MD). Slides were first changed to grey-scale images used Adobe Photoshop Elements 7.0 (Adobe Systems, San Jose, CA). The manipulated images were analyzed in Image J to determine both the area of the total infiltrate and infiltrate that exclusively contained cell types within the scala tympani. Image J measures the difference in intensities of individual pixels in a designated area on each image. A specific area, such as the scala tympani, can be sequestered from the rest of the image for analysis. Threshold for the minimum and maximum pixel size that is measured in the calculated area can be manipulated. The threshold range for the total cellular and acellular particulate infiltrate was set from 0 to 150, whereas the range for cellular infiltrate was set from

100 to 150. The measured areas in the scala tympani were compared across the three study groups.

A final score was assigned to each animal that conveyed the intensity level of the FBR in the cochlea (**Table 1**). The score was based on a previous method for determining the degree of the FBR known as Sewell's method (Black, 1999) (Sewell et al., 1955) (Gourlay et al., 1978). The scoring system was based on five measurements from our analysis. Erythrocyte cell count, neutrophil cell count, FBGC count, and fibrocyte cell count were multiplied by a weighting factor that was previously determined. The membrane width was assigned a value of 1-5 depending on the measured membrane width. The cellular response for each animal was determined by summing the total amount of cells observed and assigning this value a score of 1-5. Our scoring system and the ranges used to determine ranking were manipulated to account for the low objective we used to observe histological sections. The scores from each measurement were then summed to determine an overall ranking and intensity level of the FBR. The assigned intensity levels were very mild, mild, moderate, severe, and very severe.

Table 1.

The assigned grade with the corresponding range of the measured thickness (μm) and cellular responses is shown in top table. The cellular response is the total amount of cells within the area of the PVDF film implanted in the cochlea. The middle table depicts the weighting factor for each measurement that was incorporated into the overall intensity level of the FBR for each animal. The bottom table shows the ranges for the total score which is the sum of the five measurements in the middle table (cellular response, capsular thickness, neutrophil count, FBGC count, and fibrocyte count). Each total score range has an assigned intensity level of the FBR. The intensity levels range from the lowest level of very mild to the highest level of very severe.

TABLE 1.

Assigned Grade	Thickness Range (μm)	Cellular Response
1	0-25	0-200
2	26-50	201-400
3	51-250	401-600
4	251-500	601-800
5	501-750	801-1000

Categories	Weighting Factors
Cellular Response	x5
Capsular Thickness	x3
Neutrophil count	x5
FBGC count	x2
Fibrocyte count	x1

Score Range	Intensity level of the FBR
0-100	very mild
101-250	mild
251-500	moderate
501-600	severe
>600	very severe

III. RESULTS

There was one case of premature removal of an animal from a test group in the study. All remaining specimens did not encounter health problems and survived until the end of their predetermined time length. Necropsy results did not show signs of necrosis or infection in any of the specimens. The implant was recoverable in 17 out of 21 (81%) of the animals incorporated into our study. Statistical Analysis was conducted using SPSS (IBM, New York) and SAS (SAS Institute, North Carolina) computer software. Statistical significance was determined with a reported P-value ≤0.05.

Qualitative Analysis of Cochlear Structures

Analysis using light microscopy of the 48 hour survival length group (n=6) revealed that the PVDF film was successfully implanted in the cochlea (**Figures 5**, **6**). Cochlear structures were analyzed to determine if the structures had sustained any damage (**Table 2**). The inner and outer hair cells of the Organ of Corti had significant damage in the majority of 48 survival length group specimens. Infiltration of erythrocytes in the Organ of Corti was observed in two specimens. In each of the specimens there were exudative products as a result of hemorrhage in the scala tympani accompanying the PVDF film. The exudate was composed of erythrocytes and inflammatory cells, most notably neutrophils. Thrombocytes were observed in each implanted cochlea and angiogenesis was not evident in any of the specimens. The stria vascularis was intact in each of the specimens. Damage to the scala tympani and Reissner's membrane was observed in one specimen. Damage to the tectorial

membrane and basilar membrane was observed in two specimens. Control cochlea for the 48 hour survival length group showed exudate accumulation in the scala tympani (**Figure 7**). Aside from one animal that had major structural damage to all examined cochlear structures, control cochlea sustained a minute amount of damage to their internal structures.

The 3 week survival length group (n=7) had similar results to the 48 hour survival length group concerning the state of cochlear structures (**Figures 8**, **9**) (**Table 3**). The inner hair cells and outer hair cells of the Organ of Corti were damaged in the majority of specimens. Along with the implanted film there was a multi-layered membrane surrounding the implant. Fibrocytes were found embedded within the collagenous matrix of the formed membrane. FBGCs were observed within close proximity of the implant. Evidence of new blood vessel formation was observed in six of the specimens, while thrombocytes were observed in five of the specimens. Similar to the 48 hour survival length animals but to a lesser extent, erythrocyte accumulation as a result of hemorrhage was observed. The 3 week survival length group control (**Figure 10**) specimens had exudate in the scala tympani composed primarily of erythrocytes and thrombocytes. Damage to Organ of Corti hair cells was sustained in two control specimens.

The 3 month survival length group animals (n=4) had a multi-layered membrane formed around the implant with fibrocytes and FBGCs present (**Figure 11**). Damage was observed to inner hair cells and outer hair cells in each specimen. Thrombocytes were evident in one 3 month survival length group specimen. Angiogenesis was not evident in any of the 3 month specimens. The stria vascularis

and basilar membrane did not sustain damage for any of the 3 month specimens (**Table 4**). Thrombocytes were absent from 3 month control cochlea. Damage to the Organ of Corti was evident in two of the 3 month control cochlea (**Figure 12**).

The only measured parameter that was significantly different among the treatment groups was angiogenesis (P-value=.0002). Angiogenesis was evident only in the 3 week survival length group and absence from the 48 hour and 3 month survival length groups. A Fisher's Exact Test was conducted on each measurement to determine significance between survival length groups.

Figure 5.

10x image of implanted PVDF film (star) in scala tympani (ST) of 48 hour survival length group animal. Note the presence of exudate within the scala tympani composed of erythrocytes. Exudative products were only present in the portion of the cochlea in which the PVDF film was implanted.

Figure 5.

Figure 6.

20x image of PVDF film (Star) in scala tympani (ST). Note the exudate present composed of erythrocytes, inflammatory cells, and thrombocytes.

Figure 6.

Figure 7.

10x control cochlear image from 48 Hour survival length group animal. Note the absence of exudate from the scala tympani (ST).

Figure 7.

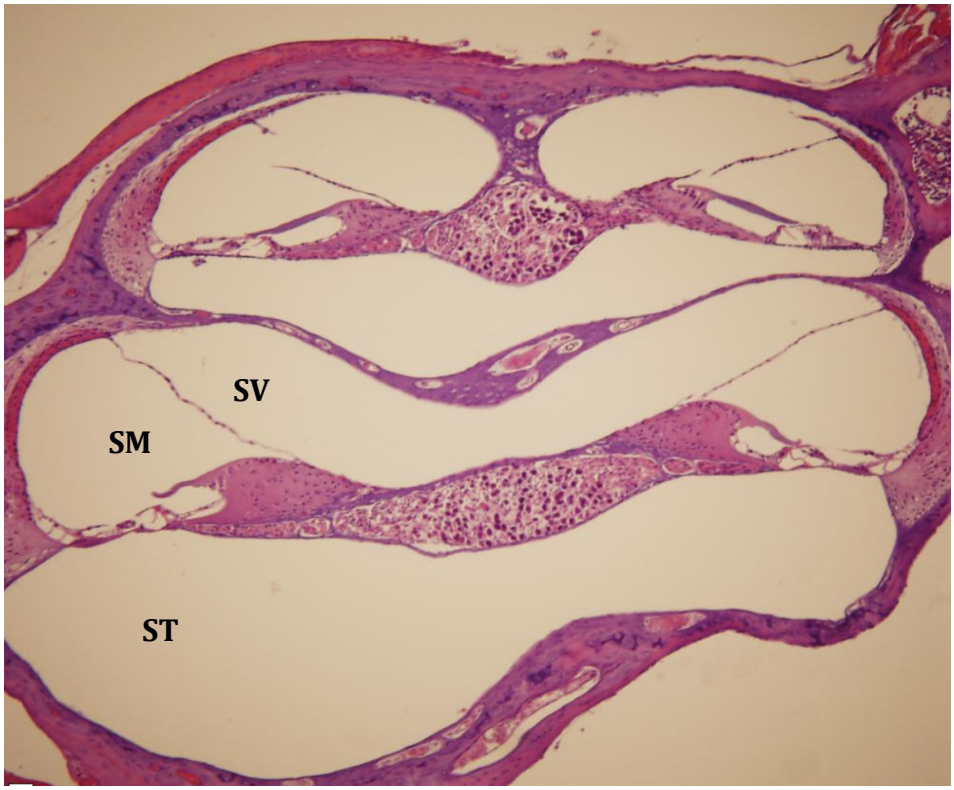

Table 2.

Condition of cochlear structures which were observed for the 48 survival length group animals. Inner and outer hair cells were damaged in the majority of implanted animals. The stria vascularis did not sustain damage in any of the implanted animals.

Table 2.

Cochlear Structure	Number of specimens with damaged structure	Number of specimens with normal structure
Basilar membrane	2	4
Outer hair cells	5	1
Inner hair cells	4	2
Tectorial membrane	2	4
Stria vascularis	0	6
Scala tympani	1	5
Reissner's membrane	1	5

Figure 8.

10x image of 3 week survival length group animal showing multi-layered membrane around PVDF film (star) in scala tympani. Note the damaged inner and outer hair cells of the Organ of Corti (black box). Fibrocytes were observed embedded in the membrane around the PVDF film (red box).

Figure 8.

Figure 9.

100x objective image of a 3 week implanted animal with PVDF film (star) in the scala tympani and foreign body giants cells (red box) present.

Figure 9.

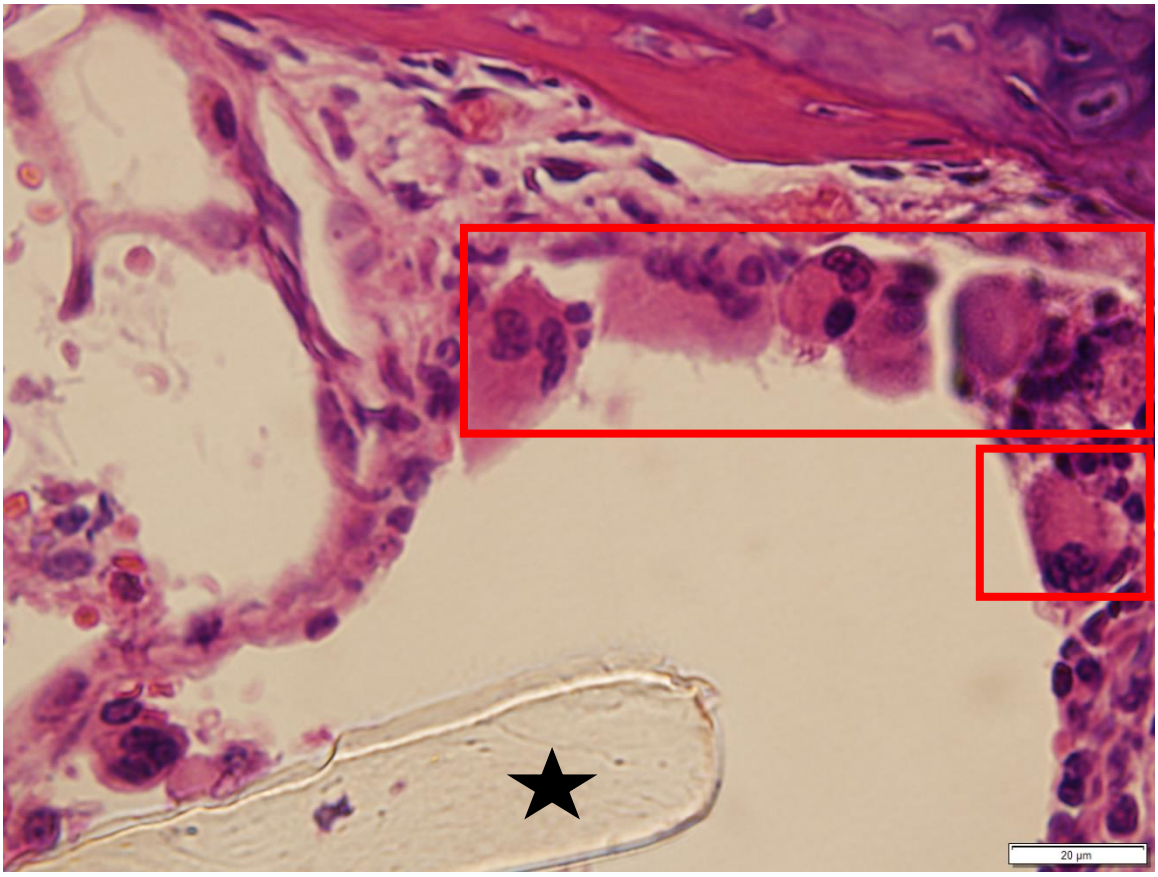

Table 3.

Conditions of cochlear structures which were observed for the 3 week survival length group animals. Outer and inner hair cells were damaged in the majority of implanted animals.

Table 3.

Cochlear Structure	Number of specimens with damaged structure	Number of specimens with normal structure
Basilar membrane	0	7
Outer hair cells	5	2
Inner hair cells	6	1
Tectorial membrane	0	7
Stria vascularis	1	6
Scala tympani	1	6
Reissner's membrane	0	7

Figure 10.

20x image of 3 week survival length group control cochlea with exudate present in scala tympani (ST). Exudative products present were composed of inflammatory cells, erythrocytes, and thrombocytes (black box). The stria vascularis (green arrow), Reissner's membrane (blue arrow), and tectorial membrane (red arrow) did not sustain damage in this specimen.

Figure 10.

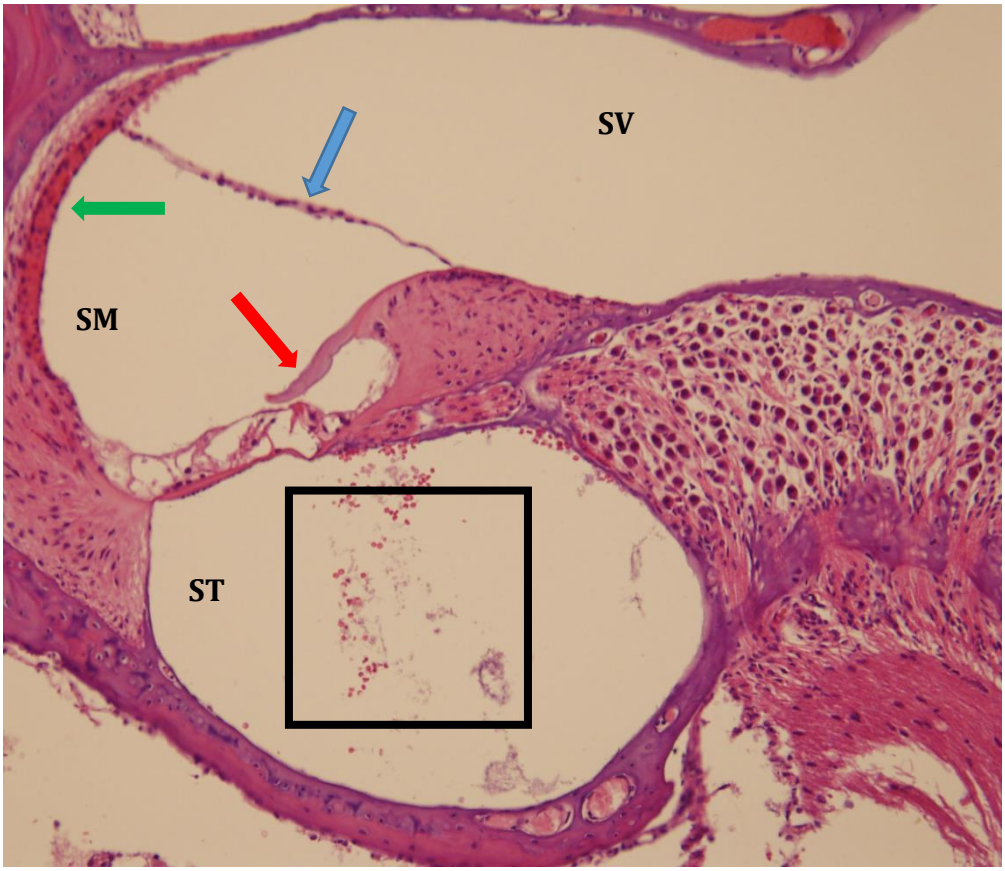

Figure 11.

20x image of 3 month survival length group animal with PVDF film (star) surrounded by a membrane in the scala tympani. Note the presence of damage to the inner and outer hair cells of the Organ of Corti (black box)

Figure 11.

Figure 12.

20x image of a control animal cochlea from the 3 month survival length group. Note the absence of damage to the inner and outer hair cells of the Organ of Corti (black box).

Figure 12.

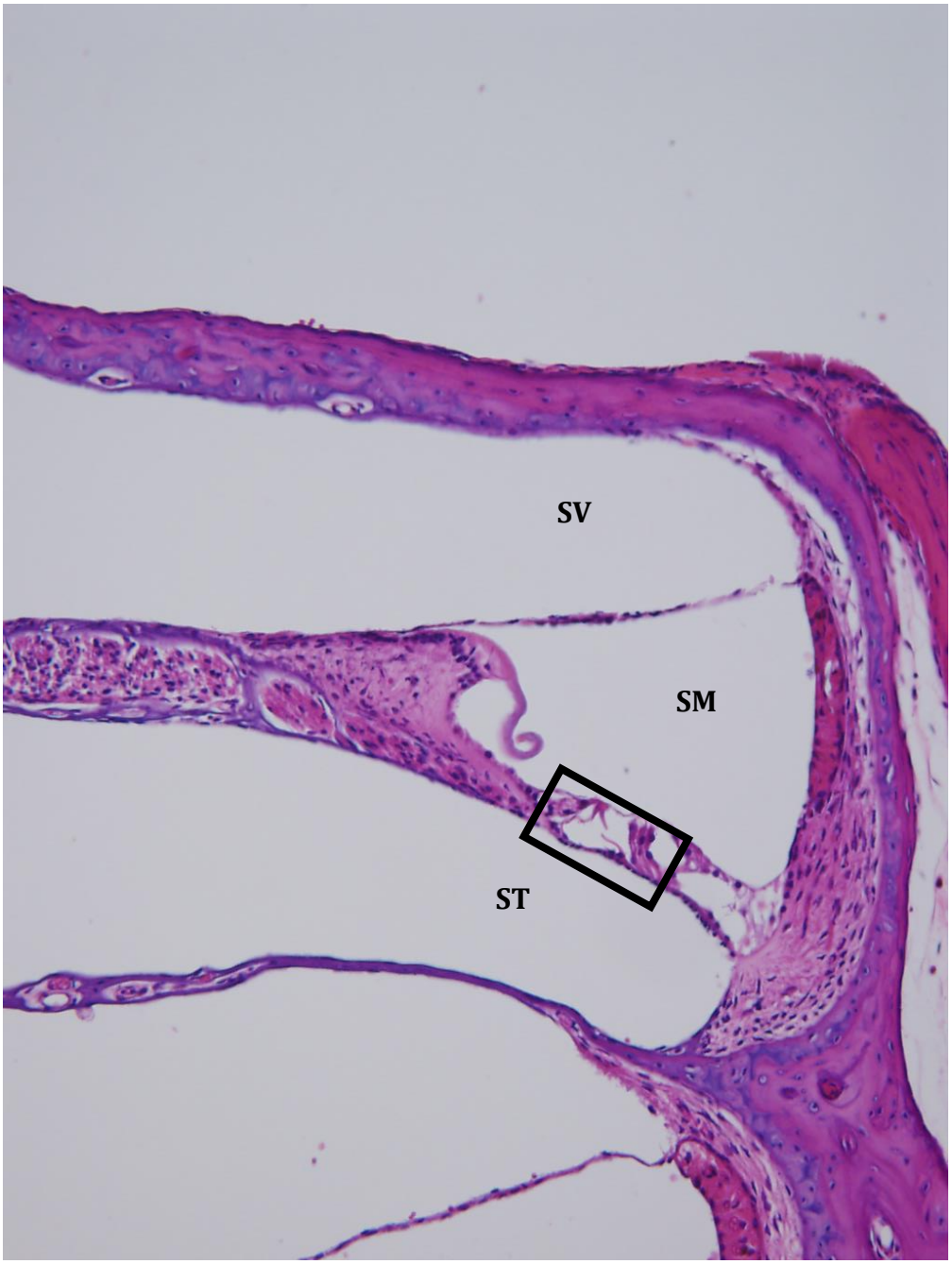

Table 4.

Condition of cochlear structures which were observed for the 3 month survival group animals. There was damage to the inner and outer hair cells of the Organ of Corti in each of the specimens. Damage to the scala tympani was evident in three of the specimens.

Table 4.

Cochlear Structure	Number of specimens with damaged structure	Number of specimens with normal structure
Basilar membrane	0	4
Outer hair cells	4	0
Inner hair cells	4	0
Tectorial membrane	2	2
Stria vascularis	0	4
Scala tympani	3	1
Reissner's membrane	0	4

Quantitative Analysis of Cochlear Exudate

The average count of cell types involved in the FBR was determined by light microscopy examination of sample slides using the 20x and 40x objectives. Statistical significance was determined using a 1-way ANOVA. Erythrocyte cell count levels (**Figure 13**) were shown to significantly decrease between the 48 hour and 3 week survival length groups (P-value=.030). The 3 month survival length group showed a slight increase in erythrocyte cell count level compared to the 3 week survival length group, but this observation was not significant. Neutrophil cell count levels (**Figure 13**) were observed at the highest intensity in the 48 hour survival length group. There was a significant decrease in neutrophil cell count levels between the 48 hour and 3 week (P-value=.022), and the 48 hour and 3 month survival length groups (P-value=.028).

Three measured parameters were observed only in the 3 week and 3 month survival length groups. Fibrocyte cell count levels (**Figure 14**) increased significantly between the 48 hour and 3 week survival length groups (P-value=0.001). FBGC levels (**Figure 15**) increased significantly between the 48 hour and 3 week survival lengths (P-value=0.001). The average membrane width around the PVDF film (**Figure 14**) increased significantly between the 48 hour and 3 week (P-value=.002) and 48 hour and 3 month (P-value=.049) survival length groups.

Figure 13.

Graph and corresponding table depicting the average cell counts for erythrocytes and neutrophils in implanted specimens and a representative control specimen.

Figure 13.

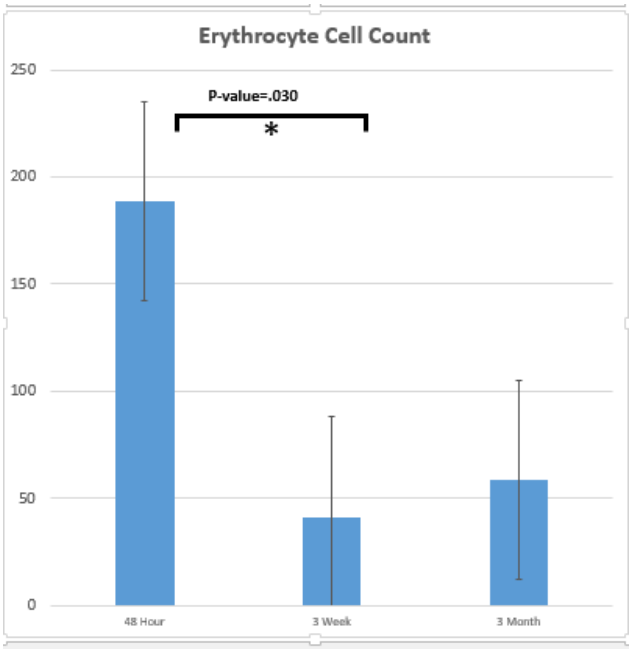

Test Group	48 Hour	3 Week	3 Month
Average	188.7	41.5	59

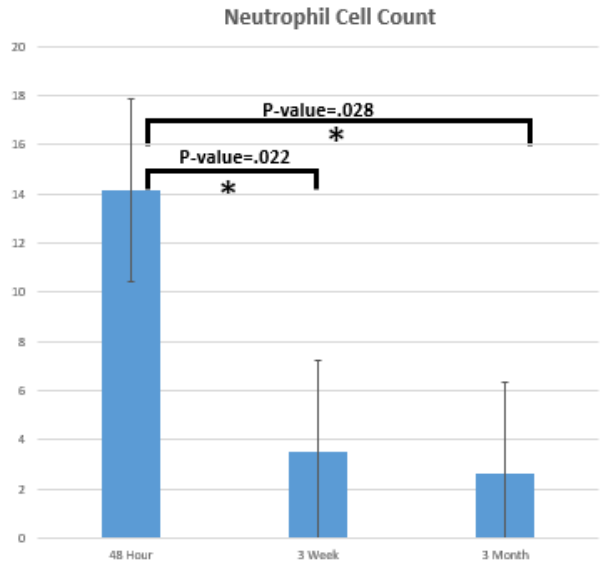

Study Group	48 Hour	3 Week	3 Month
Average	14.1	3.5	2.6

Figure 14.

Graph and corresponding table depicting the average membrane width (μm) and average cell counts for fibrocytes in implanted specimens and a representative control specimen.

Figure 14.

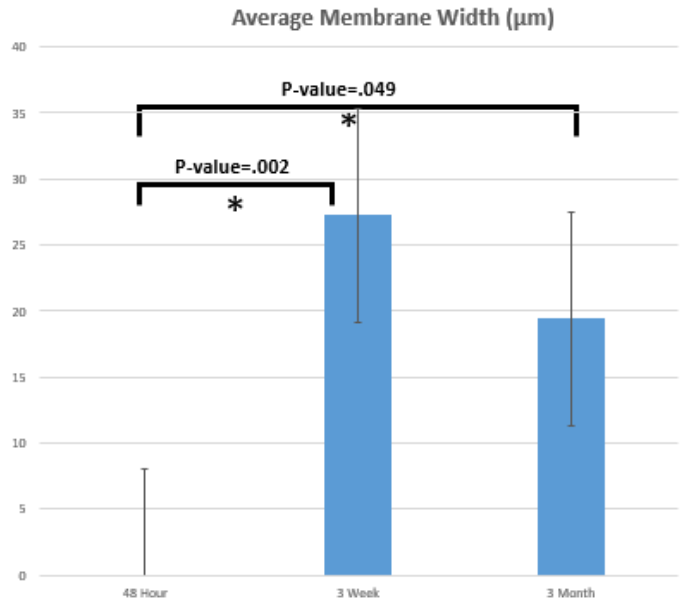

Study Group	48 Hour	3 Week	3 Month
Average	0	27.3	19.4

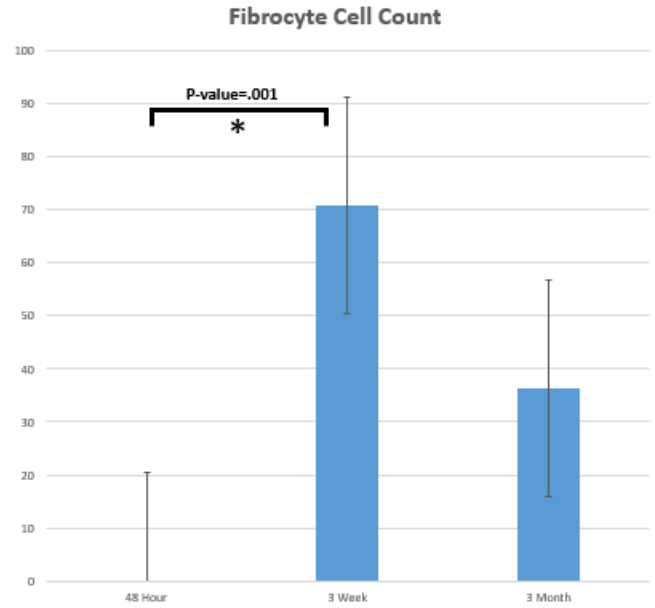

FC Data	48HR	3Week	3months
Average	0	70.75	36.4

Figure 15.

Graph and corresponding table depicting the average cell counts for FBGCs in implanted specimens and a representative control specimen.

Figure 15.

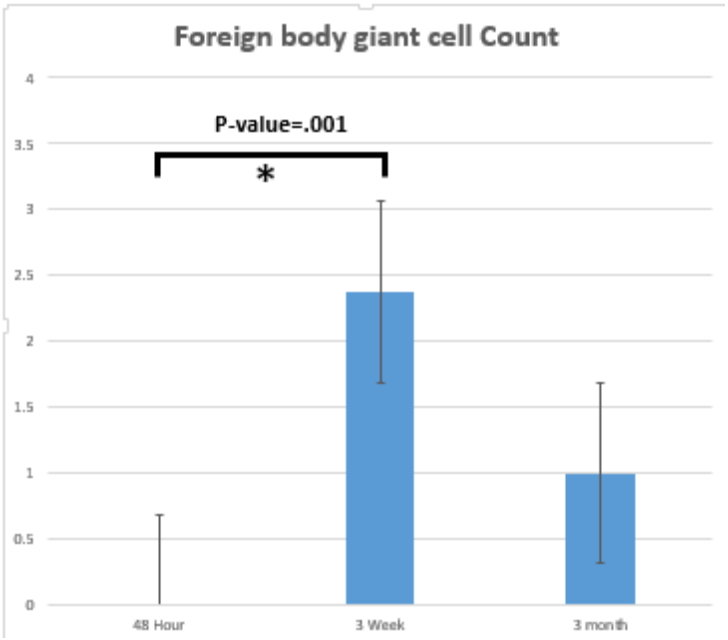

Study Group	48 Hour	3 Week	3 Month
Average	0	2.4	1

Summary of intensity levels of the FBR assigned to each animal

Five parameters were ranked for each animal to determine a final score for the FBR. This score corresponded to certain intensity level of the FBR in the cochlea. The method used to rank the FBR in this research had a range of low intensity levels (very mild and mild), a moderate intensity level, and high intensity levels (severe and very severe). The 3 week survival length group had the highest total score average of the 3 implanted test groups. There was a significant increase between the 48 Hour and 3 week time points (P-value=0.020). The majority of FBR degrees were mild with the highest intensity level observed being very mild. The Kruskal-Wallis test was used to statistically analyze the total scores of implant animals.

Figure 16.

Graph displaying the average intensity levels for the 3 survival length groups. The intensity levels of the FBR for each animals are shown in the three survival length group tables. Note that the majority of the animals had a mild intensity level of the FBR. Mild was the lowest assigned intensity level. Three of the animals in the 3 week survival length group had a very mild intensity level of the FBR.

Figure 16.

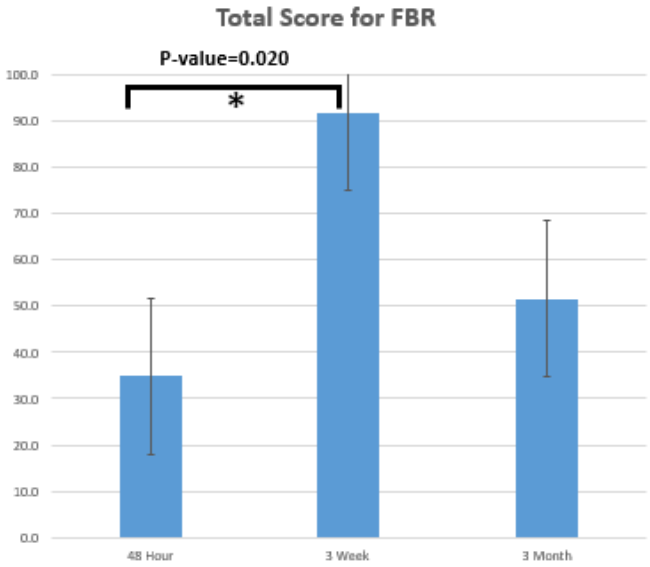

Group	48 Hour	3 Week	3 Month
Average	34.9	91.8	52

48 Hour Group.	
Intensity level	Very Mild
Score Range	0-100
48HR1	10
48HR2	11
48HR3	50
48HR4	31
48HR5	22
48HR6	68
48HR Control	52

3 Week Group.		
Intensity level	Very Mild	Mild
Score Range	0-100	101-250
3W1		162
3W2		125
3W3	95	
3W4		125
3W5	65	
3W6	65	
3W7	85	
3WControl	12	

3 Month Group.	
Intensity level	Very Mild
Score Range	0-100
3M1	50
3M2	83
3M3	61
3M4	54
3M Control	10

IV. DISCUSSION

The main objective of this research was to determine if PVDF film was biocompatible in the murine cochlea. Upon review of cochlear tissue extracted from each of the implanted animals no evidence was found of necrotic tissue or infection. The FBR observed in response to the implanted PVDF was a normal stereotypical reaction that commonly accompanies implanted biomaterials.

Summary of the measured acute responses of the FBR to PVDF film

The observed acute responses of the FBR included erythrocyte accumulation and infiltration of neutrophils around the site of implantation. Hemorrhage as a result of trauma to surrounding vasculature, vasodilation, and increase permeability of capillaries and venules leads to elevated erythrocyte cell counts at the site of implantation (Cheville, 1988). Erythrocyte cell count levels decreased significantly between the 48 hour and 3 week survival length groups. Leukocytes, most notably neutrophils, leave the vasculature during the acute phase and migrate toward the region of the implant material in response to chemotactic factors (Cheville, 1988). Neutrophil cell count levels decreased significantly between the 48 hour and 3 week survival length groups. The acute response of the FBR was a transient period that was observed in the 48 hour survival length group and did not progress into the 3 week survival length group. The neutrophil cell counts observed in each of our study groups corresponded to the inflammatory cell levels shown to accompany biocompatible materials; neutrophil presence at the site of biocompatible implants has been previously shown to resolve by 3 weeks post-implantation (Hollinger,

2012). The decrease in the amount of erythrocyte at the implant site suggests that PVDF film does not interrupt the blood coagulation and clotting mechanisms of the host. Platelets were observed at the implant site only in the test group with the highest levels of erythrocytes, the 48 survival length group. Following a traumatic event to vasculature, platelets along with plasma protein stem the flow of blood by sealing off and repairing damaged vessels (Slauson and Cooper, 1982).

Summary of the measured chronic responses of the FBR to PVDF film

The chronic phase of the FBR is characterized in part by a multi-layered membrane forming around the implanted material and the presence of fibrocytes and FBGCs (Hollinger, 2012). Our study observed these responses in the 3 week and 3 month survival length groups. There was a not a significant increase in the membrane width and presence of FBGCs and fibrocytes between the 3 week and 3 month survival length groups. The composition and integrity of the PVDF film was not affected by the chronic response of the FBR. Previous research has shown that inappropriate interfaces between implanted materials and the body can arise from allergic immune responses from the host in response to toxic or immunogenic material particulates (Hollinger, 2012). This atypical host response can result in damage and rupture to electrical leads, glucose sensors, and silicone breast implants (Hollinger, 2012).

Summary of the assigned intensity levels of the FBR

The total score for each animal also revealed that the 3 week time period contained the highest average intensity level among the three test groups. There was

a significant increase between the 48 hour and the 3 week survival length groups. The intensity of the FBR for the majority of specimens was graded at the lowest level, mild. The highest intensity of the FBR observed was very mild, which was assigned to 3 animals. These measured intensity levels of the FBR are a significant indicator of the biocompatibility of PVDF film because they reveal that both acute and chronic responses of the FBR present at the implant site of the film were at a significantly low degree over the entire time PVDF film was present in the mouse cochlea.

Summary of cochlear structural conditions and exudative area

The basilar membrane, stria vascularis, and scala tympani were intact in the vast majority of implanted animals. Upon examination of cochlear structures there was damage sustained to the inner and outer hair cells of the Organ of Corti in the majority of implanted animals. Damage to the hair cells of the Organ of Corti was also seen in the cochlea that received sham surgeries. Angiogenesis was shown to be significantly different between the three survival length group groups with it being observed only in the 3 week survival length group. Angiogenesis is a normal component of wound healing that promotes vascular growth and is present during the phase of inflammation before tissue reconstruction which leads to scar formation (Silver and Doilon, 1989).

We speculate that there are two possible sources contributing to the damaged inner and outer hair cells observed in the implanted and control cochlea. A recent study has shown that damage is sustained to the Organ of Corti when the cochlea is accessed through a round window cochleostomy (Kopelovich, 2015). Test cochlea

that received three different implant types along with sham cochlea showed damage to inner and outer hair cells. The damage to the Organ of Corti was correlated with hearing loss observed 2 weeks after the procedure (Kopelovich, 2015). Another possible source is that the strain of mice we used in the study, C57bl/6, have genetic defects that lead to hair cell degeneration. C57bl/6 mice are used in research because of their accurate depiction of age-related hearing loss. A previous study showed that hair cell degeneration is evident as early as 30 days post-partum in C57bl/6 mice (Shnerson et al., 1981). All of the animals in our study were over 30 days of age. This record of hair cell degeneration may be a possible source of the damage to hair cells recorded in our study.

Concluding remarks on biocompatibility of PVDF film

We determined the biocompatibility of PVDF film based on the observations that there was no evidence of infection or necrosis in cochlear tissue, the implant was not extruded from the cochlea, and there was not a prolonged FBR following the transient acute inflammation phase. Components of the FBR were not found in areas of the cochlea outside the site of implantation. The FBR was at the lowest possible intensity level for the majority of the time the PVDF film was implanted in the cochlea. Damage to the Organ of Corti that was observed in the majority of implanted and sham cochlea may be attributed to factors not related to the presence of the PVDF film. Chronic inflammation responses were observed in the 3 week and 3 month survival length. More notably, presence of FBGCs, fibrocytes and membrane formation have been observed around implants removed from the body.

Future Experiments

The research described in this paper can be expanded upon by identifying if a time point exists were the chronic responses of the FBR, primarily membrane formation, FBGCs, and fibrocyte presence, decrease beyond the 3 month time period. The acute response of the FBR were shown to significantly decrease at the 3 week time period, with the highest levels seen at the 48 hour time period. The only difference between this future study and the current study would be that a 4^{th} test group would be added with a survival length of 6 months.

One aspect of biocompatibility not touched upon in this research is if PVDF film is detrimental to the residual hearing in the cochlea; does the presence of the PVDF film and the resulting FBR in response to the implanted film damage the Organ of Corti, basilar membrane, or other cellular structures causing sensorineural hearing loss. This can be tested using Auditory Brainstem Responses (ABRs). An ABR is a type of auditory evoked potential that uses electrodes to measure auditory function (Willott, 2001). The recorded electrical potential can be from many different steps in the auditory pathway depending on several factors in the testing procedure, such as placement of electrodes, frequency, and wavelength measured (Willott, 2001). Baseline levels of auditory function would be measured using an external stimulus, such as a click tone, from test and sham cochlea at the start of the study. Following implantation with PVDF film, study groups would be assigned a period of 48 hours, 3 weeks, or 3 months that corresponds to the amount of time the PVDF film is inserted in the cochlea. ABRs are recorded at the end of the assigned time period for each

animal. Baseline and test ABRs are compared to observe any fluctuation or decrease in auditory function.

V. REFERENCES

Anderson, James M. "Biological Response to Materials." *Annual Review of Materials Research 31.1 (2001): 81-110*

Black, Jonathan. *Biological Performance of Materials: Fundamentals of Biocompatibility.* 3rd ed. New York: Marcel Dekker, 1999

Cheville, Norman F. *Introduction to Veterinary Pathology*. Ames, Iowa: Iowa State UP, 1988. 209-331.

Davis, J. R. "Chapter 2: Physical and Mechanical Requirements for Medical Device Materials." *Handbook of Materials for Medical Devices*. Materials Park, OH: ASM International, 2003.

Forge, Andrew, and Tony Wright. "The Molecular Architecture of the Inner Ear." *British Medical Bulletin* 63 (2002): 5-24.

Gartner, Leslie P., and James L. Hiatt. *Color Textbook of Histology*. Vol. 3. Philadelphia: W.B. Saunders, 2001. 530-36.

Gerullis, Holger, Evangelos Georgas, Mihaly Bóros, Bernd Klosterhalfen, Christoph Arndt, Stephan Otto, Dimitri Barski, Dirk Ysebaert, Albert Ramon, and Thomas Otto. "Inflammatory Reaction as Determinant of Foreign Body Reaction Is an Early and Susceptible Event after Mesh Implantation." *BioMed Research International* (2014)

Grainger, David W. "All charged up about implanted biomaterials." *Nature Biotechnology* 31 (2013): 507-509.

Goldenberg, RA and Driver, MA. Long Term Results using Hydroxlapatite Middle Ear Implants. American Journal of Otolaryngology-Head and Neck Surgery. 5:635-647. 2000

Goldenberg, Robert A., and Yan Zhuang. *Comparison of the TISHA Device to Current CI Model*. *Artificial Cochlea Research*. 2015.

Gourlay, Stuart J., Robert M. Rice, Andrew F. Hegyeli, Clarence W R Wade, James G. Dillon, Howard Jaffe, and R. K. Kulkarni. "Biocompatibility of Testing Polymers: In Vivo Implantation Studies." Journal of Biomedical Materials Research 12 (1978): 219-32.

Guyton, Arthur C., and John E. Hall. "The Sense of Hearing." *Textbook of Medical Physiology*. 11th ed. Philadelphia: Saunders, 2006. 651-61.

Hajbi-Yonissi, Carmit, Yankel Gabet, and Ralph Müller. "Nose, Palate, and Upper Jaw, Cranium and Tympanic Bulla." *Micro-tomographic Atlas of the Mouse Skeleton.* By Itai Bab. New York: Springer, 2007. 3-26.

Hollinger, Jeffrey O., ed. *An Introduction to Biomaterials*. 2nd ed. Boca Raton: Taylor & France Group, 2012.

Hu, Wen-Jing, John W. Eaton, Tatiana P. Ugarova, and Liping Tang. "Molecular Basis of Biomaterial-mediated Foreign Body Reactions."*Blood* 98 (2001): 1231-238.

Inaoka, Takatoshi, Hirofumi Shintaku, Takayuki Nakagawa, Satoyuki Kawano, Hideaki Ogita, Tatsunori Sakamoto, Shinji Hamanishi, Hiroshi Wada, and Juichi Ito. "Piezoelectric Materials Mimic the Function of the Cochlear Sensory Epithelium." *Proceedings of the National Academy of Science* 108.45 (2011).

Isaacson, Jon E., and Neil M. Vora. "Differential Diagnosis and Treatment of Hearing Loss." *American Academy of Family Physicians* 68.6 (2003): 1125-132.

Joseph, R., R. Shelma, A. Rajeev, and C.V. Muraleedharan. "Characterization of surface modified polyester fabric." *Journal of Materials Science: Materials in Medicine* (2008).

Kopelovich, Jonathan C., Barbara K. Robinson, Hakan Soken, Kristen J. Verhoeven, Jonathan R. Kirk, Shawn S. Goodman, and Marlan R. Hansen. "Acoustic Hearing after Murine Cochlear Implantation: Effects of Trauma and Implant Type." Annals of Otology, Rhinology & Laryngology (2015): 1-9.

Mistry, N., L.S. Nolan, S.R. Saeed, A. Forge, and R.R. Taylor. "Cochlear Implantation in the Mouse via the Round Window: Effects of Array Insertion." *Hearing Research* 312 (2014): 81-90.

Malhotra, Manu, Saurabh Varshney, and Rashmi Malhotra. "Cortical Bone Total Ossicular Replacement Prosthesis." *Indian Journal of Otology* 20.4 (2014): 173-77.

Monea, Monica Dana, Alexandra Stoica, Tudor Sorin Pop. "Biocompatibility of Dental Pulp Capping Materials: A Histological Study." *Acta Medica Transilvancia*. 2 (2014): 217-220

Nakagawa, Takayuki, and Juichi Ito. "Drug Delivery Systems for the Treatment of Sensorineural Hearing Loss." *Acta Oto-Laryngologica* 127 (2007): 30-35.

Nolte, John, and John W. Sundsten. "Hearing and Balance: The Eighth Cranial Nerve." *The Human Brain: An Introduction to Its Functional Anatomy*. 6th ed. St. Louis, MO: Mosby, 2009. 342-63.

Piezotech S.A.S. *Piezoelectric Films Technical Information*. Pierre-Bénite: Piezotech. *www.piezotech.fr*. Web. 19 Jan. 2015

Scudamore, Cheryl L. "Special Senses." *A Practical Guide to the Histology of the Mouse*. 1st ed. West Sussex: John Wiley & Sons, 2014. 195-210.

Sewell, William R., Wiland, Julius, and Bradford N. Craver. "A new method of Comparing Sutures of Ovine Catgut with Sutures of Bovine Catgut in three Species." Journal of Surgery, Gynecology, and Obstetrics 100.4 (1955): 483-494

Slauson, David O., and Barry J. Cooper. *Mechanisms of Disease: A Textbook of Comparative General Pathology*. Baltimore: Williams & Wilkins, 1982.

Shah, Kshitij Dhaval, Renuka A. Bradoo, Anagha A. Joshi, and Deepti D. Sapkale. "The Efficiency of Titanium Middle Ear Prosthesis in Ossicular Chain Reconstruction: Our Experience." *Indian Journal of Otolaryngology and Head and Neck Surgery* 65.4 (2013): 298-301.

Shintaku, Hirofumi, Takashi Tateno, Nobuyoshi Tsuchioka, Harto Tanujaya, Takayuki Nakagawa, Juichi Ito, and Satoyuki Kawano. "Culturing Neurons on MEMS Fabricated P(VDF-TrFE) Films for Implantable Artifical Cochlea." Journal of Biomechanical Science and Engineering 5.3 (2010): 229-35.

Shnerson, Allan, Colette Devigne, and Remy Pujol. "Age-related Changes in the C57Bl/6J Mouse Cochlea. II. Ultrastructural Findings." *Developmental Brain Research* 2 (1978): 77-88.

Silver, Frederick, and Charles Doilon. Biocompatibility Interactions of Biological and Implantable Materials. Vol. 1. New York: VCH, 1989.

Soken, Hakan, Barbara K. Robinson, Shawn S. Goodman, Paul J. Abbas, Marlan R. Hansen, and Jonathan C. Kopelovich. "Mouse Cochleostomy: A Minimally Invasive Dorsal Approach for Modeling Cochlear Implantation." *The Laryngoscope* 123 (2013): 109-15.

U.S. Food and Drug Administration. *Use of International Standard ISO-10993, Biological Evaluation of Medical Devices Part 1: Evaluation and Testing*. By Susan Alpert.*www.fda.gov/MedicalDevices*. Web. 10 Aug. 2015.

Willott, James F., ed. "Handbook of Mouse Auditory Research." *From Behavior to Molecular Biology*. New York: CRC, 2001. 37-39.

Wilson, Blake S., and Michael F. Dorman. "Cochlear Implants: A Remarkable past and a Brilliant Future." *Hearing Research* 242 (2008): 3-21.